

# Interpolation of the Josephson interaction in highly anisotropic superconductors from a solution of the two dimensional sine-Gordon equation.

Yadin Y. Goldschmidt and Sandeep Tyagi

*Department of Physics and Astronomy,*

*University of Pittsburgh, Pittsburgh, Pennsylvania 15260*

## Abstract

In this paper we solve numerically the two dimensional elliptic sine-Gordon equation with appropriate boundary conditions. These boundary conditions are chosen to correspond to the Josephson interaction between two adjacent pancakes belonging to the same flux-line in a highly anisotropic superconductor. An extrapolation is obtained between the regimes of low and high separation of the pancakes. The resulting formula is a better candidate for use in numerical simulations than previously derived formulas.

PACS numbers: 74.25.Dw, 74.25.Qt, 74.25.Ha, 74.25.Bt

## I. INTRODUCTION

High-temperature superconductors belong to the class of superconducting materials known as type II that allow for partial magnetic flux penetration whenever the external field satisfies  $H_{c1} < H < H_{c2}$ <sup>1,2,3</sup>. The flux penetrates the sample in the form of flux-lines (FL's), each containing a quantum unit  $\phi_0 = hc/2e$  of flux. At low temperature the FL's form an ordered hexagonal lattice (Abrikosov lattice) due to their mutual repulsion. At high temperature and/or magnetic field this lattice melts due to thermal fluctuations<sup>4,5,6,7,8</sup>.

High-temperature superconductors are anisotropic material which are made from stacks of superconducting layers associated with CuO<sub>2</sub> planes. The layers are weakly coupled to each other. The parameter measuring the anisotropy is  $\gamma$ , defined as  $\gamma^2 = m_z/m_{\perp}$ , where  $m_z$  and  $m_{\perp}$  denote the effective masses of electrons moving along the *c* axis (perpendicular to the superconducting planes) and the *ab* plane, respectively. While for the material YBa<sub>2</sub>Cu<sub>3</sub>O<sub>7- $\delta$</sub>  known as YBCO the anisotropy is somewhere between 5-7, for the material Bi<sub>2</sub>Sr<sub>2</sub>CaCu<sub>2</sub>O<sub>8+ $\delta$</sub>  known as BSCCO, the anisotropy is estimated to be between 10 to a 100 times larger.

For BSCCO and highly anisotropic materials similar to it, each FL is represented more faithfully by a collection of objects referred to as "pancakes". Pancakes are centered at the superconducting planes. Each pancake interacts with every other pancake, both in the same plane and in different planes. The interaction can be shown to consist of two parts. The first part is called the electromagnetic interaction (or simply magnetic) and it exists even in the case that the layers of the materials are completely decoupled, so no current can flow along the *c*-axis of the sample. A pancake vortex located in one plane gives rise to screening currents in the same plane as well as in all other planes. A second pancake vortex, located elsewhere, interacts with the screening currents induced by the first pancake<sup>9</sup>. This interaction has been calculated by Clem and others<sup>10</sup>. Two pancakes in the same plane interact with a repulsive interaction while pancakes in different planes attract one another.

The second part of the interaction among pancake vortices is the so-called Josephson interaction<sup>2,9,12</sup>. It results from the fact that there is a Josephson current flowing between two superconductors separated by an insulator and this current is proportional to the sine of the phase difference of the superconducting wave functions. The superconductors in the present case are the different CuO<sub>2</sub> planes. When two pancakes belonging to the same stack and residing in adjacent planes move away from each other, the phase difference that

originates causes a Josephson current to begin flowing between the planes. This results in an attractive interaction between pancakes that for distances small compared to  $r_g \equiv \gamma d$  is approximately quadratic<sup>2,9</sup> in the distance. When the two adjacent pancakes are separated by a distance larger than  $r_g$ , a “Josephson string” is formed, whose energy is proportional to its length<sup>12</sup>.

When doing simulations of flux lattices it is important to include correctly the strength of the interaction among pancakes. It turns out that for anisotropies smaller than about 150, the Josephson interaction is dominant over the magnetic interaction and the later can be included only in the form of an effective in-plane interaction<sup>2,13,15</sup>. For higher anisotropies the magnetic interaction must be included among all pairs of pancakes , but the Josephson interaction still matters for any finite anisotropy<sup>15</sup>. The form of the Josephson interaction used in simulation was first introduced by Ryu *et al.*<sup>13</sup> based on the Lawrence-Doniach model<sup>16</sup>. These authors used a certain approximation which can be somewhat improved. It is the aim of this paper to review the approximations made for the Josephson interaction and to suggest a better approximation to be used in numerical simulations. In order for future Monte Carlo simulations to yield a better agreement with experimental results it is important to choose the form of the interaction among pancakes to be as close as possible to the exact interaction in real materials. In the simulations the interaction among pancakes belonging to different FL's is dominantly electromagnetic for the range of magnetic fields used in experiments in the vicinity of the melting transition. For the same FL, the Josephson interaction is present predominantly for nearest neighbor pancakes which are displaced from an alignment along the z-axis. For pancakes separated by more than one plane the electromagnetic interaction is present. If a kink is present in more than one place along the same FL the total interaction is given to a good approximation as a sum of the pair interactions, provided the FL does not deviate too much from a straight line which is usually the case on the solid side of the melting line.

## II. THE MODEL

Our starting point is the Lawrence-Doniach<sup>2,16</sup> Gibbs free-energy functional,

$$\begin{aligned} \mathcal{G}[\psi_n, \mathbf{a}] = & \int d^2\mathbf{R} d \sum_n \left[ \alpha |\psi_n|^2 + \frac{\beta}{2} |\psi_n|^4 + \frac{\hbar^2}{2m} \left| \left( \frac{\nabla^{(2)}}{i} + \frac{2\pi}{\phi_0} \mathbf{a}^{(2)} \right) \psi_n \right|^2 \right. \\ & \left. + \frac{\hbar^2}{2Md^2} \left| \psi_{n+1} \exp \left( \frac{2\pi i}{\phi_0} \int_{nd}^{(n+1)d} dz a_z \right) - \psi_n \right|^2 \right] \\ & + \int d^2\mathbf{R} dz \left( \frac{b^2}{8\pi} - \frac{\mathbf{b} \cdot \mathbf{H}}{4\pi} \right), \end{aligned} \quad (2.1)$$

where  $\psi_n$  represents the superconducting order parameter in the  $n^{th}$  CuO<sub>2</sub> layer,  $\mathbf{a}^{(2)}$  is the vector potential in the plane, and  $a_z$  its component perpendicular to the planes.  $\mathbf{b}$  is the local magnetic field and  $\mathbf{H}$  is the externally applied field.  $\alpha$  and  $\beta$  are the Ginzburg-Landau parameters.  $m$  and  $M$  are the effective masses along the  $x - y$  and  $z$  directions respectively.  $d$  is the separation between the superconducting planes.  $\phi_0$  is the flux quantum. The integration along the  $z$ -direction has been replaced by a discrete summation over the superconducting layers. In the London approximation the absolute value of  $\psi_n$  is treated as a constant and its phase  $\phi_n$  is varying. The Gibbs functional becomes (dropping some constants):

$$\begin{aligned} \mathcal{G} = & \int d^2\mathbf{R} \frac{\varepsilon_0 d}{2\pi} \left\{ \sum_n \left( \nabla^{(2)} \phi_n + \frac{2\pi}{\phi_0} \mathbf{a}^{(2)} \right)^2 \right. \\ & \left. + \frac{2}{\gamma^2 d^2} \sum_n \left[ 1 - \cos \left( \phi_{n+1} - \phi_n + \frac{2\pi}{\phi_0} \int_{nd}^{(n+1)d} dz a_z \right) \right] \right\} \\ & + \int d^2\mathbf{R} dz \left( \frac{b^2}{8\pi} - \frac{\mathbf{b} \cdot \mathbf{H}}{4\pi} \right), \end{aligned} \quad (2.2)$$

where

$$\varepsilon_0 = 2\pi \frac{\hbar^2 |\psi_n|^2}{2m} = \frac{\phi_0^2}{(4\pi\lambda)^2}, \quad (2.3)$$

where  $\lambda$  is the penetration depth and and  $\gamma = \sqrt{M/m}$  is the anisotropy. Minimization with respect to  $\mathbf{a}^{(2)}$  gives

$$\lambda^2 \Delta \mathbf{a}^{(2)} = d \sum_n \delta(z - n d) \left[ \mathbf{a}^{(2)} + \frac{\phi_0}{2\pi} \nabla^{(2)} \phi_n \right], \quad (2.4)$$

where  $\Delta$  is the 3-dimensional Laplacian. Minimization with respect to  $a_z$  gives

$$\Delta a_z = \frac{4\pi}{c} j_J \sin(\Phi_{(n,n+1)}), \quad (2.5)$$

where

$$\Phi_{n+1,n} = \phi_{n+1} - \phi_n + \frac{2\pi}{\phi_0} \int_{nd}^{(n+1)d} dz a_z \quad (2.6)$$

is the gauge invariant phase difference between the layers  $n$  and  $n+1$ , and

$$j_J = \frac{c\phi_0}{8\pi^2\lambda^2\gamma^2d} \quad (2.7)$$

is the Josephson-coupling current density between layers. Minimization with respect to  $\phi_n$  gives

$$\Delta^{(2)}\phi_n + \frac{2\pi}{\phi_0} \nabla^{(2)} \cdot \mathbf{a}^{(2)} = \frac{1}{\gamma^2 d^2} [\sin(\Phi_{n,n-1}) - \sin(\Phi_{n+1,n})]. \quad (2.8)$$

We have used the Coulomb gauge  $\nabla \cdot \mathbf{a} = 0$ . Eqs. (2.4), (2.5) and (2.8) are to be solved with the appropriate boundary conditions and the solution must be substituted back into the expression for the Gibbs free-energy.

An isolated pancake residing in plane  $n$  is a singular solution of the equation for the phase of the wave function which -n the limit of  $\mathbf{R} \rightarrow \mathbf{R}_n$  satisfies

$$\nabla^{(2)}\phi_n(\mathbf{R}) = -\frac{\hat{\mathbf{z}} \times (\mathbf{R} - \mathbf{R}_n)}{(\mathbf{R} - \mathbf{R}_n)^2}, \quad (2.9)$$

where  $\mathbf{R}_n$  denotes the center of the pancake and  $\hat{\mathbf{z}}$  is a unit vector in the z-direction. This solution becomes exact in the whole plane in the infinite anisotropy limit. As one fully encircles the pancake the phase  $\phi_n$  changes by  $2\pi$ , and is singular at the center of the pancake. In the case of infinite anisotropy, the full solution of Eqs. (2.4), (2.5) and (2.8) can be found<sup>10</sup> and from it one can deduce the interaction energy for two pancakes in the same plane or in different planes. But for more complicated configurations, or when the anisotropy is finite, the solution can only be found approximately.

Consider Eq. (2.8) for the  $(n+1)$ -layer and for the  $n$ 'th layer respectively. Subtracting the second case from the first we obtain

$$\begin{aligned} & \Delta^{(2)}(\phi_{n+1} - \phi_n) + \frac{2\pi}{\phi_0} (\nabla^{(2)} \cdot \mathbf{a}^{(2)}(nd + d) - \nabla^{(2)} \cdot \mathbf{a}^{(2)}(nd)) \\ &= \frac{1}{\gamma^2 d^2} [2 \sin(\Phi_{n+1,n}) - \sin(\Phi_{n+2,n+1}) - \sin(\Phi_{n,n-1})]. \end{aligned} \quad (2.10)$$

adding and subtracting the term  $(2\pi d/\phi_0)\Delta a_z$  it becomes

$$\begin{aligned} & \Delta^{(2)}(\phi_{n+1} - \phi_n + \frac{2\pi}{\phi_0} da_z) + \frac{2\pi}{\phi_0} (-d\Delta^{(2)}a_z + d\partial_z \nabla^{(2)} \cdot \mathbf{a}^{(2)}(nd)) \\ &= \frac{1}{\gamma^2 d^2} [2 \sin(\Phi_{n+1,n}) - \sin(\Phi_{n+2,n+1}) - \sin(\Phi_{n,n-1})]. \end{aligned} \quad (2.11)$$

using the coulomb gauge we see that

$$-\Delta^{(2)}a_z + \partial_z \nabla^{(2)} \cdot \mathbf{a}^{(2)} = -(\Delta^{(2)} + \partial_z^2)a_z = -\Delta a_z. \quad (2.12)$$

We are now in a position to simplify Eq. (2.11) by using Eq. (2.6) and Eq. (2.5) together with Eq. (2.7) to finally find<sup>19,20</sup>

$$\begin{aligned} \Delta^{(2)}\Phi_{n+1,n} = & \frac{1}{\gamma^2 d^2} [2 \sin(\Phi_{n+1,n}) - \sin(\Phi_{n+2,n+1}) - \sin(\Phi_{n,n-1})] \\ & + \frac{1}{\gamma^2 \lambda^2} \sin(\Phi_{n+1,n}). \end{aligned} \quad (2.13)$$

which amazingly involves only the gauge invariant phase difference among the layers. So far this equation is nearly exact. The problem is that it represents an infinite set of coupled equations.

Consider now a FL which consists of a stack of pancakes. Assume that there is a kink in the FL in the sense that the  $n$ 'th and the  $(n+1)$ 'th pancakes are not on top of each other but are shifted a distance  $w$  along the  $x$  direction. The pancakes with index  $\geq n+1$  are all aligned along the  $z$ -direction as well as the pancakes with index  $\leq n$ . See Figure (1). In this situation one might think that except for  $\Phi_{n+1,n}$  all the phase differences vanishes. However this is not entirely true since because of the Josephson coupling there is induced phase differences away from the location of the kink. For example in the situation that  $w$  is very large a so called Josephson vortex is formed. Although its core only extends a distance  $d$  in the  $z$ -direction and a distance  $\gamma d$  in the  $y$ -direction, the associated magnetic field extends a distance  $\lambda$  in the  $z$ -direction and  $\gamma \lambda$  in the  $y$ -direction.

Nevertheless in order to truncate the infinite set of equations we will assume that we can neglect all the gauge invariant phases as compared to  $\Phi_{n+1,n}$ . This turns out to be quite satisfactory for distances much smaller than  $\gamma \lambda$ . Later we will add an overall factor to partially compensate for the approximation made. If we make this approximation, and further neglect the last term on the right hand side of Eq. (2.13) since  $\lambda^2 \gg d^2$ , we obtain<sup>17</sup>

$$\Delta^{(2)}\Phi = \frac{2}{\Lambda^2} \sin(\Phi), \quad (2.14)$$

which is the well-known elliptic sine-Gordon equation in two dimensions, where we put  $\Phi \equiv \Phi_{n+1,n}$  and  $\Lambda \equiv \gamma d$ . The energy associated with a solution to this equation due to the Josephson currents is found by evaluating the expression

$$\mathcal{G}_J = \frac{d\varepsilon_0}{\pi \Lambda^2} \int d^2\mathbf{R} (1 - \cos(\Phi(\mathbf{R}))). \quad (2.15)$$

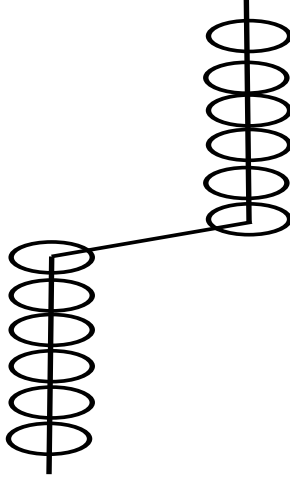


FIG. 1: A kink in a configuration of pancakes aligned along the  $z$ -direction.

The boundary conditions for the sine-Gordon equation appropriate to the configuration under discussion are fixed on the geometry depicted in Fig. (2). The outer boundary is a large circle of radius  $R_m$  which tends to infinity. On this boundary we set  $\Phi = 0$ . The inner boundary consists of two tiny circles the centers of which are a distance  $w$  apart, connected by a thin rectangle. On the inner boundary we take the solution to satisfy

$$\Phi(\mathbf{R}) = \text{atan2}(y, x - w/2) - \text{atan2}(y, x + w/2), \quad (2.16)$$

where  $\mathbf{R} = (x, y)$  and  $\text{atan2}$  is the 4-quadrant inverse tangent whose values lie in the interval  $(-\pi, \pi)$  as depicted in Fig. (3). It is to be distinguished from  $\arctan(y/x)$  whose value ie in the interval  $(-\pi/2, \pi/2)$ . Thus the values of  $\Phi$  is given approximately by the values depicted in Fig. (2). These values become exact as the radius of the inner circles and the width of the rectangle tend of zero.

We proceed by first discussing the solution under certain limiting conditions. Under these conditions we can come up with analytic expressions. One such limit is the case  $w \ll \Lambda$ . Under this condition it is a good approximation to linearize the sine-Gordon equation and solve instead the equation

$$\Delta^{(2)}\Phi = \frac{2}{\Lambda^2}\Phi, \quad (2.17)$$

which has a solution

$$\Phi(\mathbf{R}) = \frac{\sqrt{2}w}{\Lambda} \sin(\theta) K_1 \left( \frac{\sqrt{2}R}{\Lambda} \right), \quad (2.18)$$

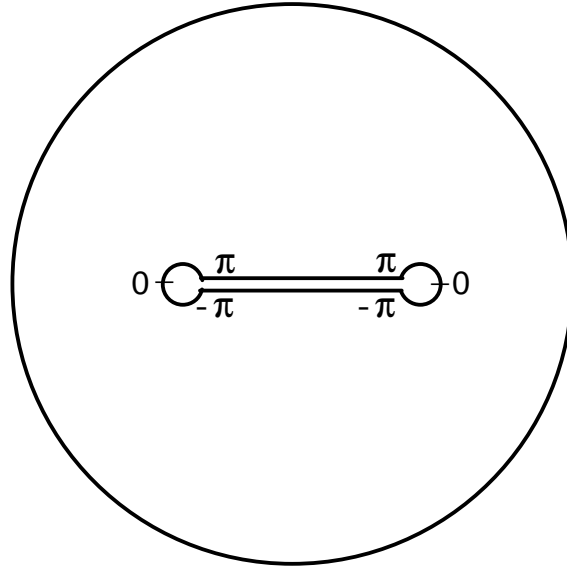


FIG. 2: Boundaries and boundary conditions for the solution of the two-dimensional elliptic sine-Gordon equation.

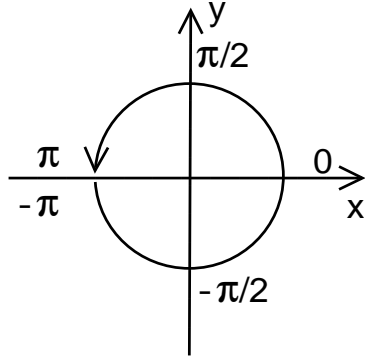


FIG. 3: definition of atan2

where  $(R, \theta)$  are the polar coordinates of the vector  $\mathbf{R}$  and  $K_1$  is the modified Bessel function of order 1. With the given boundary condition this solution is only valid for  $R \gg w$ . We see that for  $w \ll R \ll \Lambda$  the solution becomes

$$\Phi(\mathbf{R}) \sim \frac{w}{R} \sin(\theta), \quad w \ll R \ll \Lambda, \quad (2.19)$$

whereas for  $R \gg \Lambda$  we obtain

$$\Phi(\mathbf{R}) \sim \sqrt{\frac{\pi}{\sqrt{2}}} \frac{w}{\sqrt{R\Lambda}} \sin(\theta) \exp\left(-\frac{\sqrt{2}R}{\Lambda}\right), \quad R \gg \Lambda. \quad (2.20)$$

To obtain the energy we note that since  $\Phi$  is small we can expand the cosine in Eq. (2.15)

to second order in  $\Phi$  and substituting from Eq. (2.19) cutting the integration at  $w$  for lower limit and  $\Lambda$  for an upper limit we obtain for the potential energy as a function of  $w$

$$V(w) \approx \frac{\epsilon_0 dw^2}{2\pi\Lambda^2} \int_w^\Lambda \frac{dR}{R} \int_0^{2\pi} d\theta \sin^2(\theta) = \frac{\epsilon_0 d}{2} \left(\frac{w}{\Lambda}\right)^2 \ln\left(\frac{\Lambda}{w}\right) + O\left(\left(\frac{w}{\Lambda}\right)^2\right). \quad (2.21)$$

The reader may wonder how the normalization of the solution in Eq. (2.18) has been determined. This is due to the boundary conditions on the inner boundary. In the region  $w \ll R \ll \Lambda$  the term on the right hand side of Eq. (2.17) can be dropped and  $\Phi$  satisfies Laplace's equation. A solution that satisfies the boundary conditions can be written in the first quadrant in terms of the ordinary arctan function as follows:

$$\Phi(\mathbf{R}) = \arctan\left(\frac{y}{x-w/2}\right) - \arctan\left(\frac{y}{x+w/2}\right), \quad (2.22)$$

which for  $x \gg w$  gives

$$\Phi(\mathbf{R}) \approx \frac{yw}{x^2 + y^2} = \frac{w}{R} \sin(\theta), \quad (2.23)$$

in agreement with Eq. (2.19). The solution given in Eq. (2.18) matches correctly to the solution of the Laplace's equation satisfying the correct boundary conditions and hence it is properly normalized.

The other asymptotic limit that can be done analytically is the limit  $w \rightarrow \infty$ . In that limit the solution should be independent of  $x$ , and thus  $\Phi$  should satisfy the one-dimensional sine-Gordon equation

$$\frac{\partial^2}{\partial y^2} \Phi(y) = \frac{2}{\Lambda^2} \sin(\Phi(y)), \quad (2.24)$$

with the solution in the upper half plane satisfying

$$\Phi(0^+) = \pi, \quad \Phi(\infty) = 0, \quad (2.25)$$

and on the lower plane

$$\Phi(0^-) = -\pi, \quad \Phi(\infty) = 0. \quad (2.26)$$

A well-known kink solution to the sine-Gordon equation is given by

$$\Phi(y) = \text{sign}(y) \times 4 \arctan(\exp(-|y|\sqrt{2}/\Lambda)), \quad (2.27)$$

which implies

$$\sin(\Phi(y)) = 2 \sinh(y\sqrt{2}/\Lambda) / \cosh^2(y\sqrt{2}/\Lambda). \quad (2.28)$$

The energy of this solution per unit length in the  $x$  direction is given by

$$\frac{d\varepsilon_0}{\pi\Lambda^2} \int_{-\infty}^{\infty} dy \left( 1 - \cos \left( 4 \arctan(\exp(-|y|\sqrt{2}/\Lambda)) \right) \right) = \frac{4\epsilon_0 d}{\sqrt{2}\pi\Lambda}. \quad (2.29)$$

If  $w$  is large but finite, we can take the total length of the “string” as  $w$ , and to a good approximation

$$V(w) = \frac{4\epsilon_0 d}{\sqrt{2}\pi} \left( \frac{w}{\Lambda} \right), \quad w \gg \Lambda, \quad (2.30)$$

which is linear in the separation between the two singularities (pancakes). In this regime the non-linearity of the sine-Gordon equation is crucial. In the case of  $w \rightarrow \infty$ , which can be referred to as a single Josephson vortex, it is possible to find an approximate solution directly to the infinite set of equations given by Eq. (2.13). The solution found by Clem, Coffey and Hao<sup>11,12</sup> reads

$$\sin(\Phi_{n+m+1, n+m}(y)) = \frac{\Lambda}{\lambda_c^2} \frac{y K_1(r)}{r}. \quad (2.31)$$

with

$$r = \frac{\Lambda}{2\lambda_c} \left( 1 + 4y^2/\Lambda^2 + 4m^2 \right)^{1/2}. \quad (2.32)$$

where we put

$$\lambda_c \equiv \gamma\lambda, \quad (2.33)$$

The value  $m = 0$  corresponds to the position of the kink (Josephson vortex). Note that in the  $z$ -direction the phase difference decreases rapidly but not abruptly. Also there is an additional length scale  $\lambda_c \gg \Lambda$  not present in the approximation made above. If we plot the rhs of Eq. (2.31) for  $m = 0$  on the same graph as  $\sin(\Phi)$  from Eq. (2.28) for say  $\Lambda = 1$  and  $\lambda_c = 100$  we see, as depicted in Fig. (4), that both rise linearly in  $y$  up to a maximum for  $y \sim \Lambda$  and then both decay exponentially, on scales  $\lambda_c$  and  $\Lambda$  respectively. When evaluating the energy with the solution given by Eq. (2.31) one finds instead of the result represented by the rhs of Eq. (2.29) a value of

$$\left( \ln \left( \frac{\lambda_c}{\Lambda} \right) + 1.12 \right) \frac{\epsilon_0 d}{\Lambda}, \quad (2.34)$$

per unit length of the vortex in the  $x$ -direction. Using a different approximation Koshelev<sup>18</sup> claims that the constant in the last equation should be 1.55 instead of 1.12. In any case the

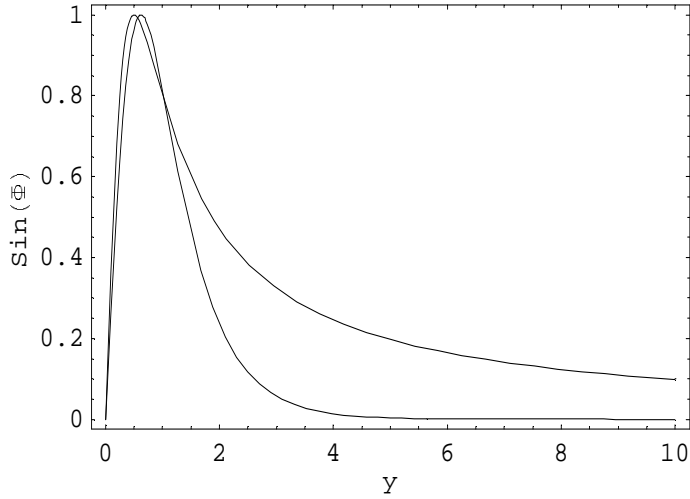


FIG. 4: Comparison of the solution given by Eq. (2.31) (longer tail) to the solution given by Eq. (2.28) plotted against  $y$  in units for which  $\Lambda = 1$  and  $\lambda_c = 100$ .

appearance of  $\ln(\lambda/d)$  is the result of the fact that the magnetic field decays over a distance of  $\lambda$  and not  $d$  in the  $z$ -direction as was implied by the neglecting the phase differences away from the  $\Phi_{n+1,n}$ . So we can correct this coefficient by introducing the logarithm by hand in front of the solution of the sine-Gordon equation as will be discussed further below.

### III. A NUMERICAL SOLUTION

The main problem is how to interpolate the potential energy of two pancakes as their separation changes from  $w \ll \Lambda$  to  $w \gg \Lambda$ . In this case an analytical solution is not available and one has to seek a numerical solution. This we achieved using the finite-element method implemented by the PDE tool of the program MATLAB. We solve the sine-Gordon equation 2.14, in the plane with the boundary condition displayed in Fig. (2) and on the inner boundary given more accurately by Eq. (2.16). We have chosen  $\Lambda = 1$ . The outer radius has been taken to be  $R_{max} = 15$  for  $0.2 \leq w \leq 10$ , and  $R_{max} = 5$  for  $w < 0.2$ . The radius of the inner circles has been taken to be  $R_{min} = 0.04$  for  $1.2 \leq w \leq 10$ ,  $R_{min} = 0.02$  for  $0.6 \leq w \leq 1.2$  and  $R_{min} = w/30$  for  $w < 0.6$ . The width of the rectangle has always been taken to be  $R_{min}/2$ .

In Figure 5 we show example of the triangular grid used for the case  $w = 10$  and the

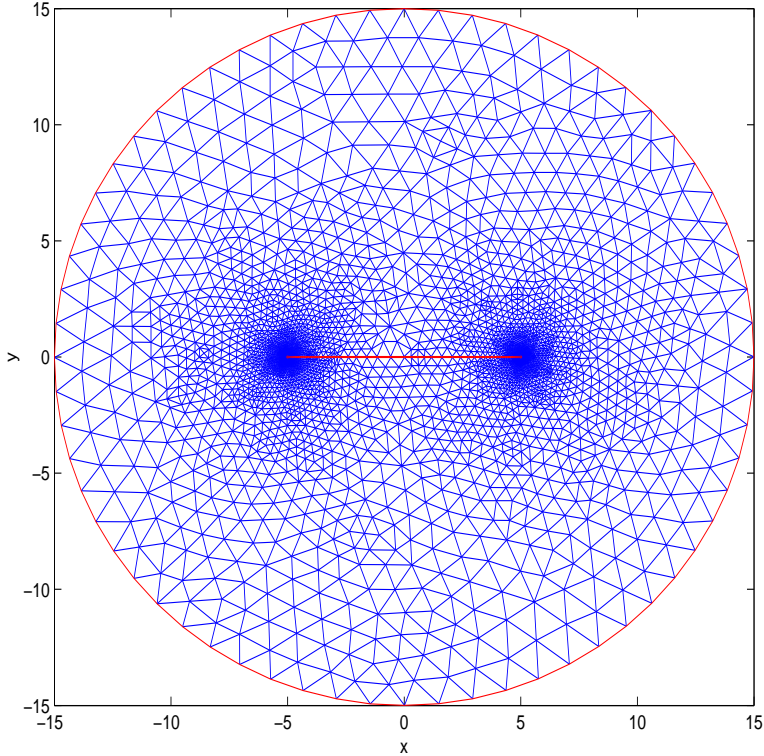


FIG. 5: Triangular grid for the case  $w = 10$ . Distances are in units of  $\Lambda$ .

corresponding solution  $\Phi(x, y)$  is depicted in Figure 6. This figure depicts contour lines of equal  $\Phi$  for some specified values as indicated in the figure caption. It can be verified that the contour lines for the range of  $x$  in the middle between the singularities ( $-3 < x < 3$ ), are almost identical to those obtained from the sine-Gordon kink solution given by Eq. (2.27) which is valid for  $w \rightarrow \infty$ . For this solution the contour lines are always parallel to the  $x$ -axis.

The energy versus pancake separation  $w/\Lambda$  is plotted in Figure 7. A good fit to the energy plot is as follows:

$$\begin{aligned}
 V &= \left(\frac{\epsilon_0 d}{\pi}\right) 0.707 \left(\frac{w}{\Lambda}\right)^2 \ln\left(\frac{9\Lambda}{w}\right), & w \leq 2\Lambda \\
 &= \left(\frac{\epsilon_0 d}{\pi}\right) \left(2.828 \left(\frac{w}{\Lambda}\right) - 1.414\right), & 2\Lambda < w,
 \end{aligned} \tag{3.1}$$

Notice that the factor  $2.828 = 4/\sqrt{2}$  agrees with the coefficient of the analytical solution given by Eq. (2.30). The prefactor of the quadratic term is smaller than that given by Eq. (2.21) since we made a fit up to a value of  $w$  larger than  $\Lambda$  in order to obtain a simpler extrapolation formula. The constant inside the logarithm captures the quadratic term on

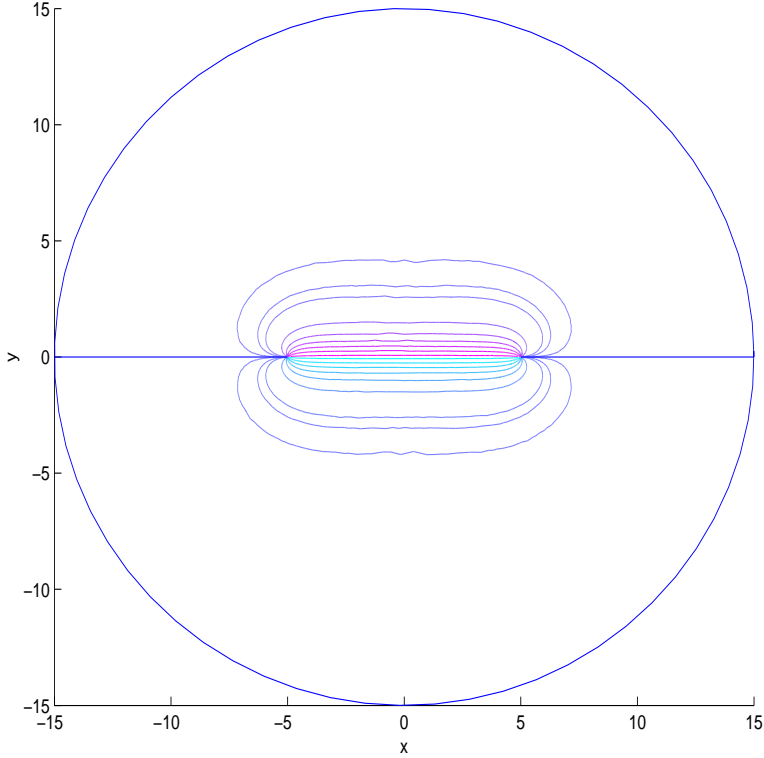


FIG. 6: Contour plot of the solution of the sine-Gordon equation for  $w = 10$ . Contour values from bottom to top: 0(boundary), -0.01, -0.05, -0.1, -0.5, -1, -1.5, -2, -2.5, -3, 3, 2.5, 2, 1.5, 1, 0.5, 0.1, 0.05, 0.01, 0 (boundary).

the right of Eq. (2.21) which is  $O((w/\Lambda)^2)$  and whose coefficient is not determined by the simple argument given. ( For very small values of  $w$  a good fit is given by  $(\pi V/\epsilon_0 d) = 1.57 (w/\Lambda)^2 \ln(2.6\Lambda/w)$  ). In order to compensate for the approximation made by the use of the sine-Gordon equation, we will now rescale the energy by a factor that will reproduce correctly the Josephson vortex energy as given by Eq. (2.34) which takes the exponential decay along the  $z$ -direction into account. Thus we suggest the following expression for the Josephson energy among two adjacent pancakes belonging to the same FL and displaced horizontally by an amount  $w$ :

$$\begin{aligned}
 V_{new}(w) &= \epsilon_0 d (1 + \ln(\lambda/d)) 0.25 (w/\Lambda)^2 \ln(9\Lambda/w), & w \leq 2\Lambda \\
 &= \epsilon_0 d (1 + \ln(\lambda/d)) ((w/\Lambda) - 0.5), & 2\Lambda < w.
 \end{aligned} \tag{3.2}$$

This expression should be compared with the extrapolation proposed by Ryu *et al.*<sup>13</sup>, that reads, after correcting for a misprint by a factor of  $2/\pi$  in that reference, and shifting by a

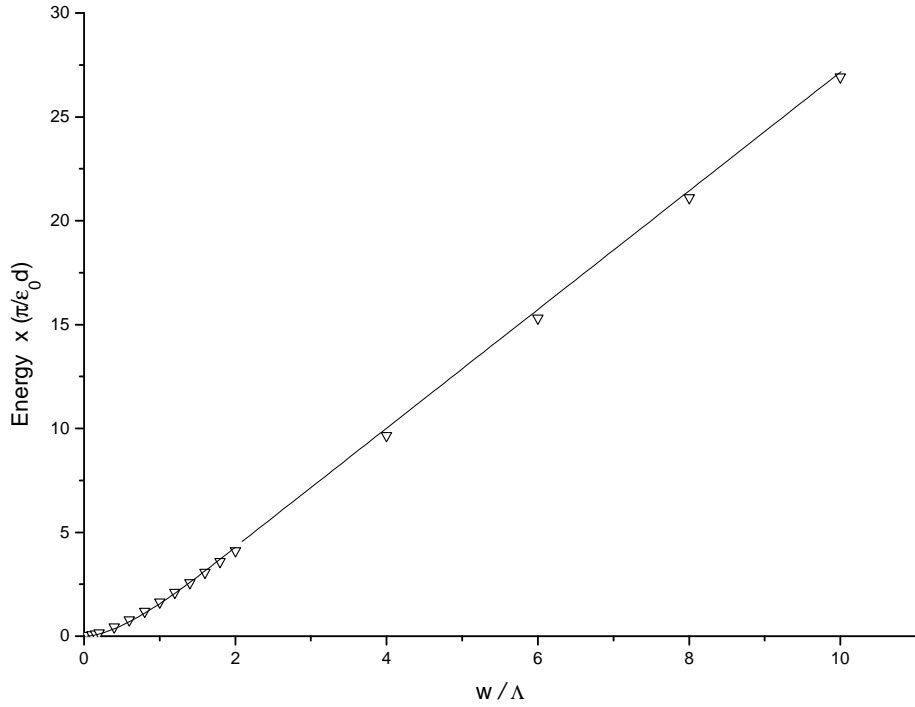


FIG. 7: The energy as obtained from the numerical solution of the sine-Gordon equation (inverted triangles) and a fit (solid line) as given by Eq. (3.1).

constant

$$\begin{aligned}
 V_{ryu}(w) &= \epsilon_0 d (1 + \ln(\lambda/d)) 0.25 (w/\Lambda)^2, & w \leq 2\Lambda \\
 &= \epsilon_0 d (1 + \ln(\lambda/d)) ((w/\Lambda) - 1), & 2\Lambda < w.
 \end{aligned} \tag{3.3}$$

These authors did not take into account the logarithmic dependence  $\ln(\Lambda/w)$  of the potential as given by Eq. (2.21) and kept only the quadratic dependence on  $w$ . They adjusted the coefficient to obtain a match of the function and its first derivative at the matching point. Note that our formula Eq. (3.2) also has the feature of a continuous first derivative (related to the force between pancakes) at the matching point. For BSCCO the value of  $\ln(\lambda/d) \approx 4.7$ . Thus the additive factor of 1 in the coefficient is rather small compared to the logarithm and this value was used by Ryu *et al.* instead of the more precise (but still approximate) value 1.12 derived in Ref. 12. Koshelev<sup>18</sup>, using a different approximation, claims that this value should actually be 1.55 and one might consider using this value instead of the additive 1 in the suggested new formula.

In Figure 8 we show a comparison of the two formulas given by Eq. (3.2) and Eq. (3.3),

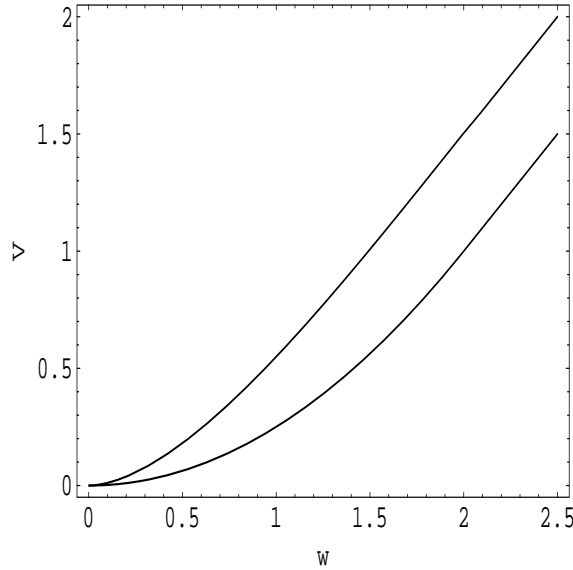


FIG. 8: Comparison of the two formulas given by Eq.(3.2) and Eq. (3.3) for  $V_{new}$  (upper curve) and  $V_{ryu}$  (lower curve) with the prefactor omitted.  $\Lambda$  was taken to be equal to 1.

where the coefficients  $\epsilon_0 d(1 + \ln(\lambda/d))$  have been omitted. The new interpolation should provide a better fit to the true potential in real systems. In the next section we discuss the results of simulations we have carried out with the new formula versus the old one.

#### IV. NUMERICAL SIMULATIONS USING THE NEW INTERPOLATION

We have carried out numerical simulations using the new formula for the Josephson interaction between pancakes. We also included the electromagnetic interaction along the lines discussed in our previous publication<sup>15</sup>. This simulation has been done with 36 planes and 36 pancakes per plane. The temperature dependence of the penetration depth used for the results displayed below is  $\lambda^2(0)/\lambda^2(T) = 1 - T/T_c$  with  $\lambda(0) = 1700$  Å,  $T_c = 90$  K and  $d = 15$  Å. The simulation method used is a multilevel Monte Carlo, as discussed in our previous publications<sup>14,15</sup>, with the only difference being the formula used for the Josephson interaction.

In Figure 9 we show the results of a simulation for BSCCO using the parameter  $\gamma = 250$  for the anisotropy and  $B = 100$  Gauss for the applied field (curves labeled as 'new'). This is to be compared with the results using the old formula for values of  $\gamma = 166$  and  $\gamma = 250$  (curves labeled as 'ryu'). It should be emphasized that the figures refer to as 'ryu' are not

results of Ryu *et. al*<sup>13</sup> but rather our simulations using their formula (corrected by a factor  $2/\pi$ ) for the Josephson interaction. The figures show the structure factor and the energy as a function of temperature. The absolute value of the energy is not meaningful since a constant has been subtracted, only energy differences are meaningful.

We see that roughly speaking the location of the melting transition for  $\gamma = 250$  using the new formula occurs at the same temperature as for  $\gamma = 166$  with the old formula, although some details like the magnitude of the structure factor and the magnitude of the energy jump are not identical so it is not just a trivial shift. The melting transition with the new formula appears a little sharper. But roughly speaking there is a scaling of the anisotropy by a factor  $\sim 1.5$  compared with using the old formula. Thus our previous estimates for the anisotropy of experimental samples should be roughly increased by this factor. In Ref. 15 we estimated the anisotropy of experimental samples used in the experiments of Majer *et al.*<sup>21</sup> to be in the range 250-450 depending on the actual temperature dependence of the penetration depth. This value should thus be increased to the range 375-675 with an average of 525. This is in good agreement with recent measurements that places the anisotropy in experimental samples to be about 550<sup>22</sup>. All the other qualitative results of our previous simulations<sup>15</sup> should remain roughly the same apart from the fact the curves should be relabeled to correspond to a higher anisotropy.

## V. CONCLUSIONS

In this paper we derived a new approximate formula for the Josephson interaction between neighboring pancakes belonging to the same flux-line. The formula extrapolates better between the limiting analytic solutions of the sine-Gordon equation than the previously derived formula by Ryu *et al.*<sup>13</sup>. We have seen that we get agreement with the experimental results of Majer *et al.*<sup>21</sup> for a value of the anisotropy  $\sim 525$  in good agreement with recent measurements of Gaifullin *et al.*<sup>22</sup> who estimate the anisotropy of their sample to be about 550.

There are still many features of BSCCO system in the presence of disorder that are not fully understood like the properties of the different phases of the vortex system found in the case of point disorder<sup>23</sup>. Future simulations to reproduce the different phases should make use of the improved formula for the Josephson interaction in order to get realistic results

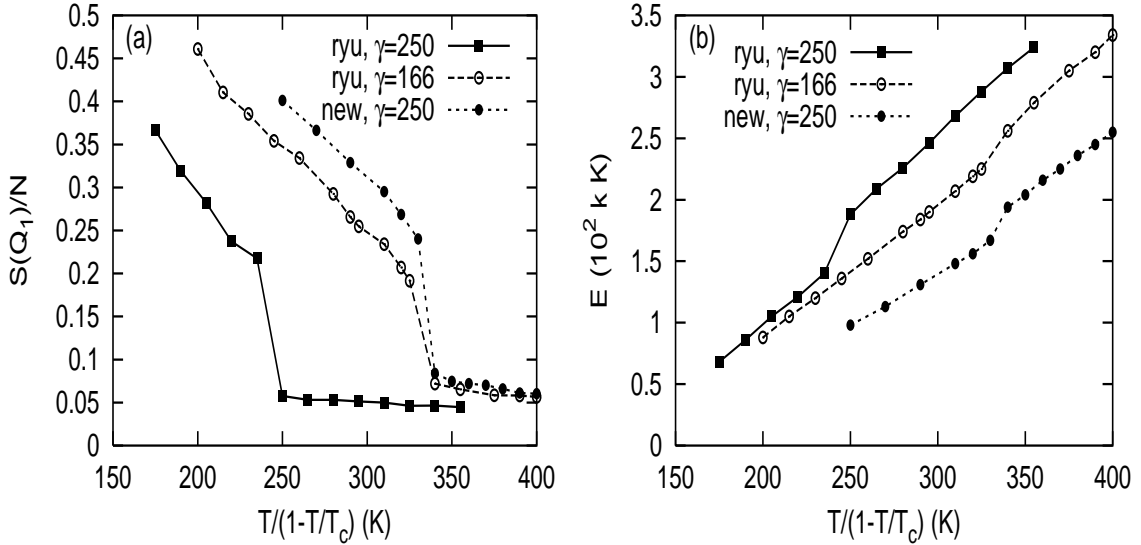


FIG. 9: Comparison of the results of multilevel Monte Carlo simulations using the new formula for the Josephson interaction as compared to the same simulations using the old formula derived by Ryu *et al.* for a magnetic field equal 100 Gauss. The electromagnetic interaction is also included. The structure factor (a) and the energy (b) are displayed.

which are in good agreement with experimental measurements.

## VI. ACKNOWLEDGMENTS

This work is supported by the US Department of Energy (DOE), Grant No. DE-FG02-98ER45686.

<sup>1</sup> M. Tinkham in *Introduction to Superconductivity*, McGraw-Hill, 1975.

<sup>2</sup> G. Blatter, M. V. Feigel'man, V. B. Geshkenbein, A. I. Larkin and V. M. Vinokur, Rev. Mod. Phys. **66**, 1125 (1994) and references therein.

<sup>3</sup> E. H. Brandt, Rep. Prog. Phys. **58**, 1465 (1995).

<sup>4</sup> H. Safar, P.L. Gammel, D.A. Huse, D. J. Bishop, J. P. Rice, and D. M. Ginsberg, Phys. Rev. Lett. **69**, 824 (1992).

<sup>5</sup> W. K. Kwok, S. Fleshler, U. Welp, V. M. Vinokur, J. Downey, G. W. Crabtree, and M. M.

Miller, Phys. Rev. Lett. **69**, 3370 (1992).

<sup>6</sup> R. Cubitt, E. M. Forgan, G. Yang, S. L. Lee, D. M. Paul, H. M. Mook, M. Yethiraj, P. H. Kes, T. W. Li, A. A. Menovsky, Z. Tarnavski and K. Mortensen, Nature **365**, 407 (1993).

<sup>7</sup> E. Zeldov, D. Majer, M. Konczykowski, V. B. Geshkenbein, V. M. Vinokur, and H. Shtrikman, Nature **375**, 373 (1995).

<sup>8</sup> A. Schilling, R. A. Fisher, N. E. Phillips, U. Welp, D. Dasgupta, W. K. Kwok, and G. W. Crabtree, Nature **382**, 791 (1996).

<sup>9</sup> S. N. Artemenko and A. N. Kruglov, Phys. Lett. A **143**, 485 (1990).

<sup>10</sup> J. R. Clem, Phys. Rev. B **43**, 7837 (1991).

<sup>11</sup> J. R. Clem and M. W. Coffey, Phys. Rev. B **42**, 6209 (1990).

<sup>12</sup> J. R. Clem, M. W. Coffey, and Z. Hao, Phys. Rev. B **44**, 2732 (1991).

<sup>13</sup> S. Ryu, S. Doniach, G. Deutscher, and A. Kapitulnik, Phys. Rev. Lett. **68**, 710 (1992); S. Ryu, Ph.D. Thesis, Stanford University (1995).

<sup>14</sup> S. Tyagi and Y. Y. Goldschmidt, Phys. Rev. B **67**, 214501 (2003)

<sup>15</sup> S. Tyagi and Y. Y. Goldschmidt, Phys. Rev. B **70**, 024501 (2004).

<sup>16</sup> W. E. Lawrence and S. Doniach, in *Proceedings of LT 12, Kyoto, 1970*, edited by E. Kanda (Keigaku, Tokyo, 1971), p. 361; S. Doniach, in *High Temperature Superconductivity, Proceedings*, edited by K. S. Bedell *et al.* (Addison-Wesley, Redwood City, 1989), p. 406.

<sup>17</sup> M. V. Feigel'man, V. B. Geshkenbein and A. I. Larkin, Physica C **167**, 177 (1990).

<sup>18</sup> A. E. Koshelev, Phys. Rev. B **48**, 1180 (1993).

<sup>19</sup> S.N. Artemenko and A.N. Kruglov, Physica C **173**, 125 (1991).

<sup>20</sup> L. N. Bulaevskii, M. Ledvij and V. G. Kogan, Phys. Rev. B **46**, 366 (1992).

<sup>21</sup> Majer, E. Zeldov, and M. Konczykowski, Phys. Rev. Lett. **75**, 1166 (1995).

<sup>22</sup> M. B. Gaifullin, Y. Matsuda, N. Chikumoto, J. Shimoyama, and K. Kishio, Phys. Rev. Lett. **84**, 2945 (2000).

<sup>23</sup> D. T. Fuchs, E. Zeldov, T. Tamegai, S. Ooi, M. Rappaport and H. Shtrikman, Phys. Rev. Lett. **80**, 4971 (1998).